Optical Engineering

OpticalEngineering.SPIEDigitalLibrary.org

Moiré apodized reflective volume Bragg grating

Sergiy Mokhov
Daniel Ott
Vadim Smirnov
Ivan Divliansky
Boris Zeldovich
Leonid Glebov

SPIE.

Sergiy Mokhov, Daniel Ott, Vadim Smirnov, Ivan Divliansky, Boris Zeldovich, Leonid Glebov, "Moiré apodized reflective volume Bragg grating," *Opt. Eng.* **57**(3), 037106 (2018), doi: 10.1117/1.OE.57.3.037106.

Moiré apodized reflective volume Bragg grating

Sergiy Mokhov,[a] Daniel Ott,[a] Vadim Smirnov,[b] Ivan Divliansky,[a] Boris Zeldovich,[a] and Leonid Glebov[a,b,*]
[a]University of Central Florida, CREOL–the College of Optics and Photonics, Orlando, Florida, United States
[b]OptiGrate Corp, Oviedo, Florida, United States

Abstract. Volume Bragg grating (VBG) with refractive index modulation (RIM) apodized with sinusoidal semiperiod profile is studied theoretically and experimentally. An apodized VBG of this type was fabricated with a sequential recording of two VBGs with slightly different resonant Bragg wavelengths in the same glass wafer. As a result, a moiré pattern was produced with a constant average refractive index and a slow sinusoidal envelope of RIM. Modeling showed that an apodized VBG with a sinusoidal semiperiod has provided a suppression of the sidelobes in the reflection spectrum. The experimental measurements are in good agreement with the theoretical predictions. This type of VBG is suitable for high-resolution spectroscopy applications due to a significant reduction of sidelobes. [DOI: 10.1117/1.OE.57.3.037106]

Keywords: volume Bragg grating; holography; apodization; moiré; spectroscopy.

Paper 171720 received Oct. 30, 2017; accepted for publication Feb. 14, 2018; published online Mar. 16, 2018.

1 Introduction

Volume Bragg gratings (VBGs) with spatially uniform refractive index modulation (RIM) are usually characterized by narrow reflection bandwidth and large aperture. VBGs fabricated in photo-thermo-refractive (PTR) glass demonstrate low optical losses and are impervious to high power laser irradiation.[1] As a result, VBGs with these advantages are used for narrowing spectra of various types of high-power lasers.[2,3] These gratings are used as well as narrow-band filters in different optical setups, and in particular, in spectroscopic applications.[4] The main quantitative characteristic of a reflective narrow-band filter is its signal-to-noise ratio (SNR) for a particular spectral range. This ratio is defined as the ratio of the maximum reflected intensity for the given spectral range to the maximum reflected intensity out of this spectral range. The reflection spectrum of a typical VBG with uniform RIM consists of a main peak with maximum reflectivity at the resonant Bragg wavelength and secondary reflection lobes decreasing rapidly with detuning from the resonant Bragg wavelength.[5] The SNR can be enhanced with sequential reflections from several uniform VBGs.[6] In this paper, we are discussing a VBG element with apodized sinusoidal RIM, which demonstrates an enhancement in the SNR in comparison with a uniform VBG.

VBGs are recorded in PTR glass by illuminating a glass wafer with periodically modulated UV light. Spatially modulated UV pattern is generated holographically by overlapping two coherent beams obtained after splitting a UV laser beam with a flat top profile. After thermal development of the exposed glass wafer, the high intensity part of the interference fringes acquires a negative refractive index change (RIC) due to photochemical processes inherent to the multicomponent PTR glass.[7] Such a standard holographic recording method provides uniform RIM inside the exposed and developed wafer. It is well-known from coupled wave theory describing the process of reflection by Bragg gratings that the apodization of the RIM leads to suppression of the secondary lobes in the reflection spectrum.[8] The apodization is represented by the smooth reduction of the amplitude of RIM from the middle of the grating to both its front and rear sides.

Fiber Bragg gratings can be straightforwardly apodized during the manufacturing process due to their simple one-dimensional geometry.[9–12] In contrast, VBGs are fabricated only by holographic recording, so the apodized profile of RIM inside the volume of a glass sample is challenging to create. One approach for apodization of VBGs is based on the recording of an interference pattern crated by the overlapping of Gaussian beams. The obtained RIM profile in this case will vary not only along the longitudinal direction but also across the aperture of the VBG, which will cause deterioration of the beam quality of the reflected beam. Also, the average background refractive index inside such VBG will vary along the longitudinal direction of the grating, which will lead to significant undesirable distortions in the reflection spectrum.[13] Another possible approach for apodization is the reduction of RIM by overexposing the front and the back areas of a VBG.[14] This method will again lead to variation of the background refractive index inside the VBG and also to the additional increase of losses in overexposed parts.

The apodization method discussed in this paper is based on sequential recording of two interference patterns with slightly different periods, with the same modulation amplitudes and with grating vectors along the same direction. As a result, a moiré pattern of RIM with constant average refractive index along the direction of beam propagation is produced. Such method of moiré apodization was implemented before for fiber Bragg gratings.[15,16] After thermal development, the apodized VBG is completed by cutting the sample to a size so it includes only one semiperiod of the RIM sinusoidal envelope. The two following sections

*Address all correspondence to: Leonid Glebov, E-mail: lbglebov@creol.ucf.edu

0091-3286/2018/$25.00 © 2018 SPIE

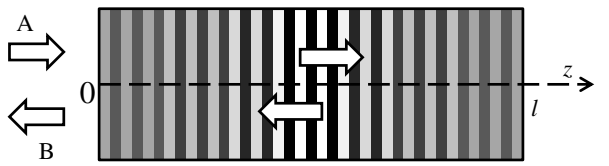

Fig. 1 Scheme of one-dimensional propagation of monochromatic incident wave A and reflected wave B in VBG with the varying amplitude $n_1(z)$ of RIM.

of the paper provide the theoretical foundations necessary for modeling the reflection spectrum of uniform and apodized VBGs. In the fourth section, our experimental results are compared with the numerical calculations.

2 Coupled Wave Theory for Bragg Reflection

The reflection of beam occurring inside VBG is described by coupled wave theory originally formulated by Kogelnik.[17] In the presented analysis, we will reproduce the main results of this theory in one-dimensional approach with wave propagation normal to the fringes of RIM inside VBG.

Let us consider a monochromatic plane wave of wavelength λ, with electric field amplitude $E(z)$, propagating in glass medium along the z-direction of a small modulation of refractive index $n(z)$. The propagation of this wave with linear polarization perpendicular to the propagation direction is described by the wave equation:

$$
\begin{aligned}
&[d^2/dz^2 + n(z)^2\omega^2/c^2]E(z) = 0, \quad \omega = 2\pi c/\lambda,\\
&n(z) = n_0 + n_1(z)\cos(Qz),\\
&|n_1(z)| \ll n_0 \;\rightarrow\; n^2(z) \approx n_0^2 + n_0 n_1(z)(e^{iQz} + e^{-iQz}). \quad (1)
\end{aligned}
$$

In the last expression, the amplitude of modulation $n_1(z)$ is assumed to be much smaller than the background refractive index of glass n_0, and the periodic RIM is presented in terms of complex waves. In case of a uniform VBG, the amplitude of RIM is constant n_1.

The electric field amplitude $E(z)$ can be represented as a sum of two counter-propagating waves with slow varying envelopes $A(z)$ and $B(z)$ (see Fig. 1):

$$
\begin{aligned}
&E(z) = [A(z)e^{ikz} + B(z)e^{-ikz}] + c.c., \quad k = n_0\omega/c,\\
&|dA/dz| \ll k|A|, \quad |dB/dz| \ll k|B|. \quad (2)
\end{aligned}
$$

Wave A is propagating in a positive z-direction since we assume the time dependence of the complex amplitude of the electric field as $\exp(-i\omega t)$. The last inequalities describe the variations of both envelopes, which are much slower than the wave oscillation itself, and they can be generalized to second-order derivatives:

$$
\begin{aligned}
&|d^2A/dz^2| \ll k|dA/dz| \ll k^2|A| \;\rightarrow\\
&\frac{d^2}{dz^2}[A(z)e^{ikz}] = e^{ikz}d^2A/dz^2 + 2ike^{ikz}dA/dz + k^2e^{ikz}A\\
&\quad \approx 2ike^{ikz}dA/dz + k^2e^{ikz}A. \quad (3)
\end{aligned}
$$

By substituting $E(z)$ in form of Eq. (2) into the wave Eq. (1) and taking into account Eq. (3), we get after simplifications:

$$
\begin{aligned}
&(2ike^{ikz}dA/dz - 2ike^{-ikz}dB/dz + c.c.) + k^2n_1(z)/n_0\\
&\quad \times (e^{iQz} + e^{-iQz})[A(z)e^{ikz} + B(z)e^{-ikz} + c.c.] = 0. \quad (4)
\end{aligned}
$$

The efficient transfer of power between the counter-propagating waves occurs in the vicinity of the Bragg resonant condition $2k = 4\pi n_0/\lambda_0 = Q$, where λ_0 is the Bragg resonant wavelength for normal incidence at a VBG with unslanted fringes. Thus, assuming $k \approx Q/2$ and assembling the terms at the corresponding oscillating factors $\exp(\pm ikz)$, we obtain a system of two coupled wave equations:

$$
\begin{aligned}
&\begin{cases} 2ie^{ikz}dA/dz + kn_1(z)/n_0B(z)e^{i(Q-k)z} = 0,\\ -2ie^{-ikz}dB/dz + kn_1(z)/n_0A(z)e^{i(k-Q)z} = 0, \end{cases} \rightarrow\\
&\begin{cases} dA/dz = i\kappa(z)B(z)e^{-2iDz}, \quad \kappa(z) = \pi\lambda^{-1}n_1(z),\\ dB/dz = -i\kappa(z)A(z)e^{2iDz}, \quad D = k - Q/2, \end{cases} \quad (5)
\end{aligned}
$$

where $\kappa(z)$ is a coupling coefficient and D is detuning coefficient. The exact resonant Bragg condition occurs at $D = 0$.

In the case of a uniform VBG with constant coupling, after proper phase redefinition of envelope amplitudes, system Eq. (5) can be represented as system of linear differential equations with constant coefficients. Introducing dimensionless coordinate $0 < \varsigma = z/l < 1$, where l is the thickness of VBG, allows the system of equations to be written in the following matrix form:

$$
\begin{aligned}
&\frac{d}{d\varsigma}\begin{pmatrix} a\\ b \end{pmatrix} = \begin{pmatrix} i\Phi & iS\\ -iS & -i\Phi \end{pmatrix}\begin{pmatrix} a\\ b \end{pmatrix},\\
&a = Ae^{i\Phi\varsigma}, \quad b = Be^{-i\Phi\varsigma}, \quad \varsigma = z/l, \quad S = \kappa l = \pi n_1 l/\lambda_0,\\
&\Phi = Dl = 2\pi n_0 l(\lambda^{-1} - \lambda_0^{-1}) = -2\pi n_0 l\lambda_0^{-2}(\lambda - \lambda_0). \quad (6)
\end{aligned}
$$

Here, two dimensionless parameters are introduced: the strength of reflection S and the phase detuning Φ. Since we are studying the narrow spectral region of strong coupling, $\lambda \approx \lambda_0$, we used the value of resonant Bragg wavelength λ_0 in the definition of S, and Φ was rewritten to be proportional to the wavelength shift.

The solution of the linear differential system in Eq. (6) with constant coefficients is known in analytical form.[18] In terms of amplitudes A and B, it is

$$
\begin{aligned}
&\begin{pmatrix} A_l\\ B_l \end{pmatrix} = \hat{M}\begin{pmatrix} A_0\\ B_0 \end{pmatrix}, \quad \hat{M} = \begin{pmatrix} e^{-i\Phi} & 0\\ 0 & e^{i\Phi} \end{pmatrix}\begin{pmatrix} m_{11} & m_{12}\\ m_{21} & m_{22} \end{pmatrix},\\
&m_{22} = m_{11}^* = \cosh G - i\frac{\Phi}{G}\sinh G,\\
&m_{21} = m_{12}^* = -i\frac{S}{G}\sinh G, \quad G = \sqrt{S^2 - \Phi^2}. \quad (7)
\end{aligned}
$$

Here, A_0 and B_0 are the amplitude values at the front side of the VBG at $z = 0$ and A_l and B_l are the amplitude values at the back side of the VBG at $z = l$.

The amplitude reflection coefficient r is defined as the ratio of the reflected amplitude B_0 to the incident amplitude A_0 with the assumption of no wave B entering the grating from the rear side, $B_l = 0$. We assume VBG with anti-reflection-coated surfaces, so Fresnel reflections are not

considered. As a result, the condition $B_l = M_{21}A_0 + M_{22}B_0 = 0$ for the second equation in Eq. (7) provides the following analytical expressions for the reflection coefficient and the reflectivity R:

$$r = \frac{B_0}{A_0}\Big|_{B_l=0} = -\frac{M_{21}}{M_{22}} = \frac{iS/G \sinh G}{\cosh G - i\Phi/G \sinh G},$$

$$R = |r^2| = \frac{\sinh^2\sqrt{S^2-\Phi^2}}{\cosh^2\sqrt{S^2-\Phi^2} - \Phi^2/S^2}. \quad (8)$$

We have obtained the formula for the reflection spectrum $R(\lambda)$ of a uniform Bragg grating, which depends on the grating parameters n_0, n_1, λ_0, and l in accordance with Eq. (6).

At the exact Bragg resonance $\Phi = 0$, the reflectivity equals $R_0 = \tanh^2 S$. At the spectral edge of the reflection band $\Phi = S$, the expression for reflectivity in Eq. (8) resolves to $R(\Phi = S) = S^2/(1+S^2)$. In the next section, we will make a comparison between the reflection spectrum of a uniform VBG and the reflection spectrum of an apodized VBG.

3 Theoretical Modeling of Apodized Volume Bragg Grating

The PTR glass is photosensitive to UV exposure at wavelength $\lambda_{UV} = 325$ nm. After UV exposure with a given dosage and a thermal development, RIC of up to 2000 ppm (0.002) in PTR glass can be achieved. Applying a particular thermal treatment regime and using small exposure dosages, a linear dependence of the RIC from the dosage is observed, whereas with significant increase of the dosage, RIC starts to saturate to its maximum achievable value. The dependence of the RIC on dosage is described actually by saturation curve of hyperbolic type.[19] For recording VBGs, the UV light is modulated along a single direction with a period corresponding to the desired resonant Bragg wavelength λ_0. Such modulation is formed holographically by overlapping two coherent UV waves as we mentioned before.

Let us consider two coherent UV waves with wavevectors $\mathbf{k}_1$ and $\mathbf{k}_2$, propagating in plane with z-axis and x-axis oriented, as shown in Fig. 2. These waves are incident on a glass sample with front surface plane at $x = 0$. If these UV waves have TE polarization and angle of incidences α, then the created interference pattern in space is described by a phase function $\Psi(z)$, which is the same in glass or air due to phase-matching conditions at the air–glass boundary:

$$\mathbf{k}_{1,2} = 2\pi\lambda_{UV}^{-1}(\pm\mathbf{e}_z \sin\alpha - \mathbf{e}_x \cos\alpha),$$
$$|e^{i\mathbf{k}_1\mathbf{r}} + e^{i\mathbf{k}_2\mathbf{r}}|^2 = 2(1+\cos\Psi),$$
$$\Psi = (\mathbf{k}_1 - \mathbf{k}_2)\mathbf{r} = 4\pi\lambda_{UV}^{-1} z \sin\alpha. \quad (9)$$

Exposure with such interference pattern transfers as a periodic modulation of the dosage gained by the glass over the time of UV exposure. This dosage modulation will be imprinted as RIM defined by $\cos(Qz)$ in Eq. (1) after the thermal treatment in the regime of linear photosensitivity. So, according to the resonant Bragg condition $D = 0$ in Eq. (5), the incidence angle α required in holographic setup for recording VBG with resonant Bragg wavelength λ_0 is determined as follows:

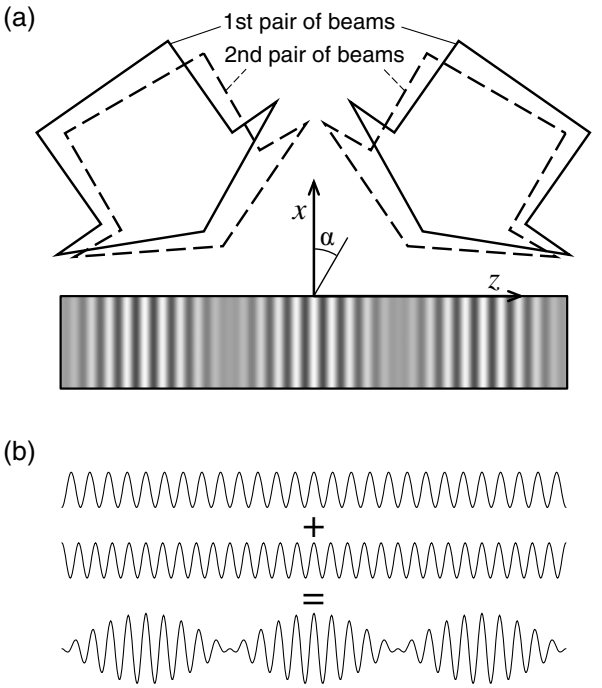

Fig. 2 (a) Recording of moiré pattern of RIM inside PTR glass sample by using two sequential holographic UV exposures. (b) Formation of the moiré pattern by overlapping two uniform periodic patterns with slightly different periods.

$$Qz = \Psi = 4\pi\lambda_{UV}^{-1} z \sin\alpha,$$
$$D = 0 = 2\pi n_0\lambda_0^{-1} - Q/2 \;\rightarrow\; \alpha = \arcsin(n_0\lambda_{UV}/\lambda_0). \quad (10)$$

Two sequential holographic UV exposures of specimen with slightly different modulation periods will create a moiré pattern of dosage, which produces corresponding moiré pattern of RIM inside the glass.

The two modulations defined by resonant Bragg wavelengths λ_1 and λ_2 with small difference $\Delta\lambda$ between them and with the same modulation amplitude n_1 will create moiré pattern with parameters following from a well-known trigonometric identity illustrated in Fig. 2(b):

$$\cos\alpha + \cos\beta = 2\cos[(\alpha+\beta)/2]\cos[(\alpha-\beta)/2],$$
$$n_1\cos(Q_1 z) + n_1\cos(Q_2 z) = N_1\cos(qz)\cos(Qz),$$
$$N_1 = 2n_1, \quad Q_{1,2} = 4\pi n_0/\lambda_{1,2}, \quad \Delta\lambda = \lambda_2 - \lambda_1 \ll \lambda_{1,2},$$
$$\lambda_0 \cong (\lambda_1+\lambda_2)/2, \quad Q = 4\pi n_0/\lambda_0, \quad q = 2\pi n_0\Delta\lambda/\lambda_0^2. \quad (11)$$

Here, λ_0 is the resonant Bragg wavelength of the combined moiré pattern equal to the average of the two close to each other particular Bragg wavelengths, where q is the wavector of the slow periodic envelope of the moiré pattern.

The thickness l_m of the VBG with RIM apodized by semiperiod of the moiré envelope is determined according to Eq. (11) by the semiperiod π-phase condition:

$$ql_m = 2\pi n_0\Delta\lambda l_m/\lambda_0^2 = \pi \;\rightarrow\; l_m = \lambda_0^2/(2n_0\Delta\lambda). \quad (12)$$

The necessary wavelength difference $\Delta\lambda$ is determined by predefined thickness l_m of an apodized VBG, and the required difference $\Delta\alpha$ between angles of the two holographic recordings can be derived from Eq. (10).

The apodized RIM $n_{1m}(z)$ along the semiperiod of the moiré pattern is defined according to Eqs. (11) and (12):

$$n_m(z) = n_0 + n_{1m}(z)\cos(Qz),$$
$$n_{1m}(z) = N_1 \sin(\pi z/l_m), \quad 0 \le z \le l_m. \tag{13}$$

For convenience of notations, here, we have introduced the semiperiod as sin-function for $n_{1m}(z)$ instead of cos-function as in Eq. (11).

For an apodized VBG, coupled wave equations in Eq. (5) contain a varying ampliude $n_{1m}(z)$ of RIM from Eq. (13):

$$\begin{cases} dA/dz = i\kappa_m(z)B(z)e^{-2iDz}, & 0 \le z \le l_m, \\ dB/dz = -i\kappa_m(z)A(z)e^{2iDz}, & \kappa_m(z) = \pi\lambda_0^{-1}n_{1m}(z), \end{cases}$$
$$n_{1m}(z) = N_1 \sin(\pi z/l_m), \qquad D = 2\pi n_0(\lambda^{-1} - \lambda_0^{-1}). \tag{14}$$

By using dimensionless coordinate $0 < \varsigma = z/l_m < 1$ and performing phase redefinition of the envelope amplitudes A and B, coupled wave equations in Eq. (14) can be represented in modified form similar to Eq. (6):

$$\frac{d}{d\varsigma}\begin{pmatrix} a \\ b \end{pmatrix} = \begin{bmatrix} i\Phi & iS_m(\pi/2)\sin(\pi\varsigma) \\ -iS_m(\pi/2)\sin(\pi\varsigma) & -i\Phi \end{bmatrix}\begin{pmatrix} a \\ b \end{pmatrix},$$
$$a = Ae^{i\Phi\varsigma}, \quad b = Be^{-i\Phi\varsigma}, \quad S_m = 2N_1 l_m/\lambda_0, \quad \varsigma = z/l_m,$$
$$\Phi = Dl_m = -2\pi n_0 l_m \lambda_0^{-2}(\lambda - \lambda_0). \tag{15}$$

Here, the dimensionless phase detuning Φ is the same as in Eq. (6). We also introduced the dimensionless strength of reflection S_m, which is convenient for describing the reflection by an apodized VBG, especially in the case of exact Bragg resonance $\Phi = 0$.

Since the coefficients of the linear differential equations system in Eq. (15) are not constant, specifically, off-diagonal coupling terms are varying as sin-function; there is no analytical solution for this system. Only at the exact Bragg resonance $\Phi = 0$, the system Eq. (15) can be integrated analytically. The propagation matrix in this case, for amplitudes A and B determined at the incident side of the apodized VBG, $z = 0$, and at the back side, $z = l_m$, is as follows:

$$\Phi = 0: \begin{pmatrix} A_{l_m} \\ B_{l_m} \end{pmatrix} = \begin{pmatrix} \cosh S_m & i\sinh S_m \\ -i\sinh S_m & \cosh S_m \end{pmatrix}\begin{pmatrix} A_0 \\ B_0 \end{pmatrix}, \tag{16}$$

where S_m is defined in Eq. (15).

Reflectivity of an apodized VBG at the exact Bragg resonance is calculated using the same boundary condition $B_{lm} = 0$ as in Eq. (8) and applied now to Eq. (16):

$$\Phi = 0: \quad r = \left.\frac{B_0}{A_0}\right|_{B_{lm}=0} = \frac{i\sinh S_m}{\cosh S_m}, \quad R_0 = |r^2| = \tanh^2 S_m. \tag{17}$$

In the case of arbitrary wavelength detuning $\Phi \neq 0$, the reflectivity R can be obtained by numerically calculating the propagation matrix similarly to (7,8). This matrix follows from numerical integration of the system of equations in Eq. (14) or the equivalent system in Eq. (15):

$$\begin{pmatrix} a_1 \\ b_1 \end{pmatrix} = \begin{pmatrix} m_{11} & m_{12} \\ m_{21} & m_{22} \end{pmatrix}\begin{pmatrix} a_0 \\ b_0 \end{pmatrix}:$$
$$\begin{pmatrix} a_0 \\ b_0 \end{pmatrix} = \begin{pmatrix} 1 \\ 0 \end{pmatrix} \rightarrow \begin{pmatrix} m_{11} \\ m_{21} \end{pmatrix} = \begin{pmatrix} a_1 \\ b_1 \end{pmatrix};$$
$$\begin{pmatrix} a_0 \\ b_0 \end{pmatrix} = \begin{pmatrix} 0 \\ 1 \end{pmatrix} \rightarrow \begin{pmatrix} m_{12} \\ m_{22} \end{pmatrix} = \begin{pmatrix} a_1 \\ b_1 \end{pmatrix}. \tag{18}$$

The propagation matrix $\hat{m}$ transforms amplitudes a and b at the front side of grating with $\varsigma = 0$ to amplitudes at the back side with $\varsigma = 1$. Starting with the initial conditions $a_0 = 1$ and $b_0 = 0$, integration of the system of differential equations in Eq. (15) provides amplitudes a_1 and b_1 equal to the corresponding matrix elements m_{11} and m_{21} according to Eq. (18). Similarly, integration of Eq. (15) with initial conditions $a_0 = 0$ and $b_0 = 1$ provides matrix elements m_{12} and m_{22}.

The calculated matrix elements of the propagation matrix $\hat{m}$ for a particular wavelength λ determine the amplitude reflection coefficient r and the reflectivity R using the condition of absence of wave B at the end of the grating, $b_1 = 0$, which was already used in Eq. (8) for the case of a uniform grating:

$$b_1 = m_{21}a_0 + m_{22}b_0 \rightarrow r = \left.\frac{B_0}{A_0}\right|_{B_{lm}=0} = \left.\frac{b_0}{a_0}\right|_{b_1=0} = -\frac{m_{21}}{m_{22}},$$
$$R = |r^2| = \left|\frac{m_{21}}{m_{22}}\right|^2. \tag{19}$$

Figure 3 shows the reflection spectrum $R(\Phi)$ numerically calculated in accordance with (15,18,19) for apodized VBG with maximum resonant reflectivity $R_0 = 99\%$. The corresponding strength of reflection based on Eq. (17) is $S_m = 2.99$. The dimensionless detuning parameter Φ can be expressed through the wavelength shift for the particular grating. For example, if the background refractive index is $n_0 = 1.485$, the resonant Bragg wavelength is $\lambda_0 = 1.064\ \mu$m, and the thickness of the VBG l_m is 5 mm, then, according to the definition of Φ in Eq. (15), the wavelength shift equals $\lambda - \lambda_0 = -24.3 \cdot \Phi$ pm. For such parameters λ_0 and l_m, according to Eq. (15), the maximum amplitude of apodized RIM required to obtain the mentioned S_m is $N_1 = 318$ ppm. Figure 3 also presents the spectrum of a uniform VBG calculated from the analytical expression Eq. (8) with the same maximum reflectivity $R_0 = 0.99$ and correspondingly the same value of $S = 2.99$. For the same n_0, λ_0, $l = l_m$, the detuning parameter Φ has the same definition for both apodized (15) and uniform (6) types of VBGs, and the wavelength shift $\lambda - \lambda_0$ depends on Φ in the same manner mentioned above.

The reflection spectrum of an apodized VBG demonstrates significant suppression of secondary lobes in comparison with the spectrum of a uniform volume grating. Precise cutting of the sample at the exact locations of moiré envelope zeros is crucial for fabricating of apodized VBG. If the cut is not properly done at the zeros of the envelope, then the achieved apodization would not be accurate and the reflection spectrum will show higher secondary

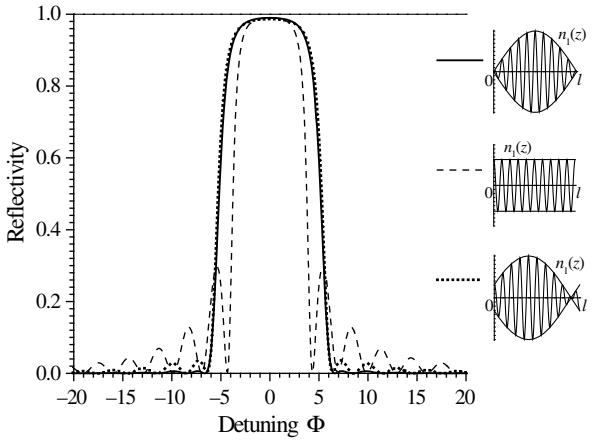

Fig. 3 Dependence of reflectivity R on dimensionless detuning Φ for different VBGs: apodized VBG (solid line), uniform VBG with the same maximum reflection 99% (dashed line), and apodized VBG with 10% cut mismatch in the apodization profile (dotted line).

parasitic lobes. In order to demonstrate this effect of inaccurate apodization, in Fig. 3, we have included the spectrum of a VBG with the same length l_m of the moiré semiperiod but with 10% relative mismatch in the locations of envelope zeros. The corresponding RIM of this flawed apodized VBG is described by $n_{1m}(z) = N_1 \sin[\pi(z/l_m + 0.1)]$, having the additional term of 0.1 in comparison to the flawless apodization description given by Eq. (14).

From Fig. 3, we can see that the width of the main reflection peak of an apodized VBG is wider than the main peak of a uniform VBG. This is because the effective thickness of an apodized VBG is smaller than the thickness l of a uniform VBG. It is well-known that the reflection bandwidth of a Bragg grating is inversely proportional to its length. This basic fact can be proven from the mathematical expression for detuning $|\Phi| = 2\pi n_0 l(\lambda - \lambda_0)/\lambda_0^2$ from Eq. (6). For detuning value $|\Phi| = S = 2\pi n_0 l \Delta\lambda_S/\lambda_0^2$ with corresponding wavelength shift $\Delta\lambda_S$, the reflectivity is equal to $R_S = S^2/(1 + S^2)$, as it was mentioned in Eq. (8). This reflectivity value R_S for grating with larger l will be achieved at smaller wavelength shift $\Delta\lambda_S$ in order to keep the same detuning value $|\Phi| = S$. So, the larger peak width of an apodized VBG in comparison with the peak width of a uniform VBG with the same thicknesses $l = l_m$ can be explained actually by the smaller effective thickness of the apodized VBG. For the presented spectra with 99% maximum reflectivity, the FWHM width of the apodized VBG is $\Delta\Phi_{FWHM,m} = 10.35$, at the level of 49.5%. This width is 1.37 times larger than the width of $\Delta\Phi_{FWHM} = 7.53$ of the uniform VBG, which is also equal to $\Delta\lambda_{FWHM} = 183$ pm if using the modeling numerical parameters n_0, l, λ_0 mentioned earlier. Despite of the larger width of the main reflection peak, the apodized VBG could be more suitable for spectroscopic measurements. In spectroscopic applications, the main design goal is to achieve the best SNR over certain bandwidth using a narrow-band filter, and in this sense, the apodized VBG with significantly suppressed parasitic secondary lobes of reflection demonstrates better performance than the ordinary uniform VBG.

In our theoretical analysis, we considered the propagation of incident and reflected waves along the same z-direction normal to the planes of RIM fringes and VBG surfaces. In the case of skew incidence at a small angle θ_{air} to the normal of the VBG surface, the incident wave will propagate inside VBG glass medium at a refracted angle θ_{in}. Thus, the Bragg resonant condition defined by zero detuning $D = 0$ pointed out below Eq. (5) should be adjusted by substituting the wavevector k by its z-component k_z. This will lead to maximum reflectivity at a new resonant wavelength λ_{res} slightly different from the Bragg wavelength λ_0 for normal incidence:

$$D = k_z - Q/2 = 0, \quad k_z = 2\pi n_0 \lambda_{res}^{-1} \cos\theta_{in} \rightarrow$$
$$\lambda_{res} = \lambda_0 \cos\theta_{in} \approx \lambda_0(1 - \theta_{in}^2/2) = \lambda_0[1 - \theta_{air}^2/(2n_0^2)]. \tag{20}$$

So, the wavelength of resonant Bragg reflection λ_{res} can be slightly decreased by angular detuning from normal incidence. With such angular detuning, the maximum reflectivity will not change significantly, because the coupling parameter $\kappa(z)$ in Eq. (5) should be divided by $\cos\theta_{in}$ and, in the case of TM polarization, additionally multiplied by $\cos(2\theta_{in})$.

4 Experimental Reflection Spectrum of Apodized VBG

Our initial experiments with moiré patterns in PTR glass dealt with the reflection and transmission properties of moiré VBG with a full period of the slow sinusoidal envelope of RIM.[20,21] Two envelope semiperiods of such VBG contain an intrinsic π-phase shift between them. At Bragg resonant wavelength, this VBG system behaves in a way similar to a Fabry–Perot filter, and it demonstrates a very narrow transmission peak with bandwidth of tens of pm. In this paper, we are presenting the results for a moiré VBG with only one semiperiod of the sinusoidal envelope profile of RIM. The main objective of studying this apodized VBG is to demonstrate the enhanced suppression of secondary lobes in the reflection spectrum if compared to a similar uniform VBG.

To create an apodized VBG, a PTR glass specimen was sequentially exposed with two UV interference patterns according to the schematic illustration in Fig. 2. Each pattern was designed to have a uniform RIMs with a resonant Bragg wavelengths close to $\lambda_0 = 1.064$ μm. The background refractive index of the PTR glass at wavelength λ_0 is $n_0 = 1.485$. Typical thicknesses of high-aperture uniform reflective VBGs used in spectroscopy applications are 2 to 5 mm. The change $\Delta\alpha$ of the angle of holographic recording presented in Fig. 2 was made at the minimum achievable level of 0.1 mrad in our experiment. According to Eq. (10), this value corresponding to the small difference $\Delta\lambda$ between the resonant wavelengths equals approximately 200 pm, and the corresponding semiperiod l_m was estimated to be less than 2 mm from Eq. (12). The sample was thermally developed to imprint the moiré pattern created by double UV exposure into a permanent moiré pattern of RIM. The semiperiod l_m of the fabricated slow moiré envelope was determined by testing the Bragg diffraction in transmission regime using an argon ion laser operating at 488 nm. The longitudinal periodicity of the intensity of the transmitted light directly corresponds to l_m. The measured value of the semiperiod was $l_m = 1.635$ mm. An apodized VBG with a thickness of l_m was then cut from the wafer.

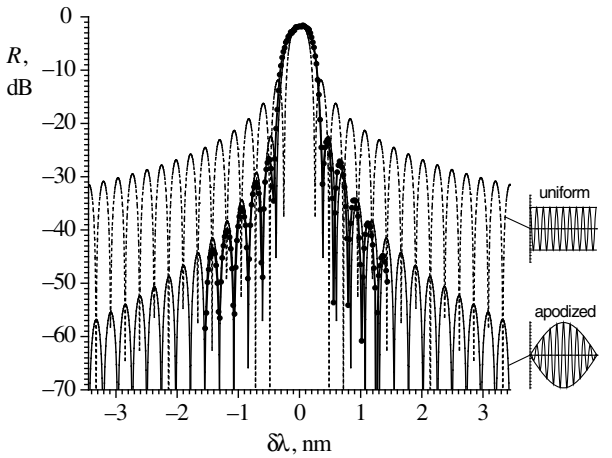

Fig. 4 Experimental reflection spectrum of apodized VBG (dots connected by thick line), its theoretical fit (thin line), and theoretical reflection of referent uniform VBG (dashed line).

The reflection spectrum of the apodized VBG with antireflection coated surfaces was measured with a tunable laser source with beam diameter 1 mm and subpicometer linewidth. Figure 4 shows the experimental reflection spectrum in logarithmic scale along with the associated theoretical curve. The maximum value of the RIM of the moiré envelope defined in Eq. (11) was determined to be $N_1 = 430$ ppm by matching the response from the theoretical fit. The strength of reflection is $S_m = 1.32$ according to Eq. (15), which gives a maximum of reflectivity $R_0 = \tanh^2 S_m = 75\%$. Figure 4 also includes the modeling of a reflection spectrum of a uniform VBG with the same parameters $S = S_m$, n_0, λ_0, and $l = l_m$.

The use of a logarithmic scale in Fig. 4 clearly shows the enhanced suppression of secondary lobes in the spectrum of an apodized VBG in comparison with lobes in spectrum of a similar uniform VBG. In case of the apodized VBG, SNR is equal to 45 dB over a 3-nm spectral range with the maximum reflectivity in the middle of it, whereas in the case of a uniform VBG, SNR is equal to 25 dB over the same spectral range. Our experimental measurements are in good agreement with theoretical simulations.

It is instructive to provide analytical estimations for the decrease of reflectivity as a function of wavelength detuning for both apodized and uniform VBGs. At large wavelength detuning, when the wavelength λ of the incident wave is very far from the Bragg resonant wavelength λ_0, the reflection value R, which defines the intensity of the reflected wave B, is very small. Therefore, we can apply the Born approximation to the system of coupled differential equations in Eq. (5) for a uniform VBG, or to the system Eq. (14) for an apodized VBG. In this approximation, the incident wave A is considered not to be disturbed, so $B = 0$ is assumed in the differential equation for A, and we have to find the solution for the generated wave B from its corresponding differential equation consisting of the already known expression for the undisturbed wave A. With this approximation, system Eq. (5) is simplified to one differential equation for B. As a result, with a boundary condition at the rear side of the grating $B(l) = 0$ already discussed above for a wave reflected from the front side of grating, we obtain reflectivity R_u of a uniform VBG in the Born approximation:

$$A(z) = A(0): \quad dB/dz = -i\kappa A(0)e^{2iDz},$$

$$B(l) = 0 \;\rightarrow\; B(z) = +i\kappa A(0)\int_z^l e^{2iDz'}\mathrm{d}z',$$

$$r_u = B(0)/A(0) = i\kappa\int_0^l e^{2iDz}\mathrm{d}z = ie^{i\Phi}S/\Phi\cdot\sin\Phi,$$

$$R_u = S^2/\Phi^2\cdot\sin^2\Phi, \quad \langle R_u\rangle = S^2/(2\Phi^2). \tag{21}$$

The definitions of the dimensionless detuning Φ and the strength of reflection S are specified in Eq. (6). Equation (21) represents the averaged expression $\langle R_u\rangle$ of reflectivity over several periods of Φ, and it was obtained by substituting the periodic factor $\sin^2\Phi$ with its average value of ½. These results show that the reflectivity of a uniform VBG decreases with detuning as Φ^{-2}.

Similarly, we can find asymptotic behavior of the reflectivity of an apodized VBG when operating at a large out-of-Bragg resonance detuning. By applying the Born approximation to system Eq. (14), which means the amplitude of wave A is kept unchanged, we can find the approximate solution for small amplitude of the reflected wave B. The boundary condition $B(l_m) = 0$ leads to amplitude reflection coefficient and reflectivity of an apodized VBG:

$$A(z) = A(0): \quad \frac{d}{dz}B = -i\frac{\pi N_1}{\lambda_0}\sin\left(\frac{\pi z}{l_m}\right)A(0)e^{2iDz},$$

$$B(l_m) = 0 \rightarrow B(z) = i\frac{\pi N_1}{\lambda_0}A(0)\int_z^{l_m}\sin\left(\frac{\pi z'}{l_m}\right)e^{2iDz'}\mathrm{d}z',$$

$$r_m = \frac{B(0)}{A(0)} = i\frac{\pi N_1}{\lambda_0}\int_0^{l_m}\sin\left(\frac{\pi z}{l_m}\right)e^{2iDz}\mathrm{d}z = \frac{-i\pi^2 S_m e^{i\Phi}\cos\Phi}{4\Phi^2-\pi^2},$$

$$R_m = \frac{\pi^4 S_m^2\cos^2\Phi}{(4\Phi^2-\pi^2)^2}, \quad \langle R_m\rangle = \frac{\pi^4 S_m^2}{2(4\Phi^2-\pi^2)^2}. \tag{22}$$

The strength of reflection S_m of an apodized VBG is defined in Eq. (15). R_m is the reflectivity of an apodized VBG in the Born approximation, and $\langle R_m\rangle$ is the value with averaging of the periodic factor $\cos^2\Phi$. Thus, for an apodized VBG, the asymptotic dependence of reflectivity from wavelength detuning is proportional to Φ^{-4}. This power dependence provides very fast reduction of the secondary reflection lobes in comparison with the dependence Φ^{-2} obtained previously for an ordinary uniform VBG.

Successive reflection of a laser beam by a pair of uniform VBGs is determined by the product of two reflectivities of individual gratings, and the total reflectivity is described by asymptotic dependence Φ^{-4} similar to the reflectivity of apodized VBG. The enhancement of spectral selectivity by utilization of one apodized VBG instead of consecutive implementation of two uniform VBGs preserves the robustness of optical setup.

5 Conclusions

We presented the coupled wave equations necessary for the theoretical modeling of the reflectivity of apodized VBGs produced by holographic recording of moiré patterns and derived asymptotic formulas for the decrease of the reflectivity for both uniform and apodized VBGs as the wavelength of an incident beam is detuned far from the resonant wavelength. The reflectivity of the uniform grating decreases inversely proportional to the square of the detuning while

the reflectivity of an apodized grating decreases inversely proportional to the fourth power of detuning. An apodized VBG was manufactured based on the moiré principle by recording two uniform gratings with slightly different periods in one wafer. The apodized grating demonstrated efficient suppression of secondary lobes in the reflection spectrum. The fabricated apodized VBG had resonance at 1064 nm, was 1.6 mm long, had 75% maximum reflectivity, and showed 45-dB suppression in side lobe reflectivity over 3-nm spectral range centered at the resonant wavelength. By comparison, the standard uniform VBG with the same thickness and maximum reflectivity provides only 25-dB contrast over the same 3-nm spectral range. The experimental results were in good agreement with the numerical calculations. The results summarized above demonstrate that an apodized grating is compact and robust optical element with superior side lobe suppression in comparison with compound schemes based on a pair of uniform gratings providing the same level of contrast.

References

1. L. Glebov, "Volume holographic elements in a photo-thermo-refractive glass," *J. Hologr. Speckle* **5**, 77–84 (2009).
2. B. V. Zhdanov et al., "Continuous wave Cs diode pumped alkali laser pumped by single emitter narrowband laser diode," *Rev. Sci. Instrum.* **86**, 083104 (2015).
3. G. Venus et al., "Spectral narrowing and stabilization of interband cascade laser by volume Bragg grating," *Appl. Opt.* **55**, 77–80 (2016).
4. V. Smirnov et al., "Ultra-narrow line filters with enhanced transmittance for low-frequency Raman spectroscopy," in *Conf. on Lasers and Electro-Optics* (2016).
5. H. Shu et al., "More on analyzing the reflection of a laser beam by a deformed highly reflective volume Bragg grating using iteration of the beam propagation method," *Appl. Opt.* **48**, 22–27 (2009).
6. D. Ott et al., "High-contrast filtering by multipass diffraction between paired volume Bragg gratings," *Appl. Opt.* **54**, 9065–9070 (2015).
7. J. Lumeau and L. Glebov, "Effect of the refractive index change kinetics of photosensitive materials on the diffraction efficiency of reflecting Bragg gratings," *Appl. Opt.* **52**, 3993–3997 (2013).
8. R. Kashyap, *Fiber Bragg Gratings*, 2nd ed., pp. 189–216, Academic Press, Burlington, Massachusetts (2009).
9. J. Albert et al., "Apodisation of the spectral response of fibre Bragg gratings using a phase mask with variable diffraction efficiency," *Electron. Lett.* **31**, 222–223 (1995).
10. A. Asseh et al., "A writing technique for long fiber Bragg gratings with complex reflectivity profiles," *J. Lightwave Technol.* **15**, 1419–1423 (1997).
11. C. Martinez, S. Magne, and P. Ferdinand, "Apodized fiber Bragg gratings manufactured with the phase plate process," *Appl. Opt.* **41**, 1733–1740 (2002).
12. R. J. Williams et al., "Point-by-point inscription of apodized fiber Bragg gratings," *Opt. Lett.* **36**, 2988–2990 (2011).
13. V. Mizrahi and J. E. Sipe, "Optical properties of photosensitive fiber phase gratings," *J. Lightwave Technol.* **11**, 1513–1517 (1993).
14. J. M. Tsui et al., "Coupled-wave analysis of apodized volume gratings," *Opt. Express* **12**, 6642–6653 (2004).
15. S. Legoubin et al., "Formation of moiré grating in core of germanosilicate fibre by transverse holographic double exposure method," *Electron. Lett.* **27**, 1945–1947 (1991).
16. H.-G. Froehlich and R. Kashyap, "Two methods of apodisation of fibre Bragg gratings," *Opt. Commun.* **157**, 273–281 (1998).
17. H. Kogelnik, "Coupled wave theory for thick hologram gratings," *Bell Syst. Tech. J.* **48**, 2909–2947 (1969).
18. L. Glebov et al., "Reflection of light by composite volume holograms: Fresnel corrections and Fabry-Perot spectral filtering," *J. Opt. Soc. Am. A* **25**, 751–764 (2008).
19. J. Lumeau and L. Glebov, "Modeling of the induced refractive index kinetics in photo-thermo-refractive glass," *Opt. Mater. Express* **3**, 95–104 (2013).
20. V. Smirnov et al., "Ultranarrow bandwidth moiré reflecting Bragg gratings recorded in photo-thermo-refractive glass," *Opt. Lett.* **35**, 592–594 (2010).
21. S. Mokhov et al., "Moiré volume Bragg grating filter with tunable bandwidth," *Opt. Express* **22**, 20375–20386 (2014).

Sergiy Mokhov was graduated from the Department of Theoretical Physics of Kiev University in Ukraine in 1996. Then, he pursued his PhD in nuclear physics at that university. In 2004, he moved to CREOL—the College of Optics at the University of Central Florida. Since 2006, he has worked with Professor B. Zeldovich and Professor L. Glebov's group on the theory of volume Bragg gratings. He earned his PhD in optics from CREOL in 2011.

Daniel Ott received his BS degree in optical engineering from Rose-Hulman Institute of Technology and later his PhD in optics from the College of Optics at the University of Central Florida in 2014 for work in holographic recording of multiplexed VBGs in PTR glass. After graduation, he joined the Surface and Nanostructure Metrology Group at the National Institute of Standards and Technology as a postdoctoral fellow researching pattern recognition algorithms for forensic ballistic identification.

Vadim Smirnov received his MS degree in optics at CREOL, University of Central Florida, in 2000. He is a cofounder, director of holography, and chief technology officer at OptiGrate Corp. He is the coauthor of more than 100 presentations and publications and three U.S. patents on high-efficiency diffractive elements in photo-thermo-refractive glass. His research activities include design and fabrication of volume diffractive gratings and holograms, nonlinear phenomena in optical glasses, and laser design.

Ivan Divliansky received his PhD degree in electrical engineering/materials science from The Pennsylvania State University in State College, Pennsylvania, United States, in 2004. Since 2007, he has been a senior research scientist at CREOL, the College of Optics and Photonics at the University of Central Florida in Orlando. His current research interests include high-power laser beam combining, diode and fiber lasers systems design, implementation of volume Bragg gratings in different photonics areas, vector beam generation, and others.

Boris Zeldovich graduated from Moscow University in 1966 and received his doctor of physical and mathematical sciences degree from Lebedev Physics Institute in Moscow, Russia. He is currently a professor of optics and physics at the University of Central Florida's CREOL College of Optics and Photonics. He is the codiscoverer of optical phase conjugation. He is a member of the Russian Academy of Science and won the 1997 Max Born award for physical optics from OSA.

Leonid Glebov received his PhD degree from the State Optical Institute, Leningrad, Russia (1976). He is a research professor at CREOL/UCF and cofounder and VP at OptiGrate Corp. He is a coauthor of a book, more than 300 papers, and 10 patents. He is a fellow of ACerS, OSA, SPIE, and NAI. He is a recipient of the Gabor award in holography. His main directions of research are optical properties of glasses, holographic optical elements, and lasers.